APPLICATION OF ARTIFICIAL NEURAL NETWORK FOR THE DIRECT ESTIMATION OF ATMOSPHERIC INSTABILITY FROM A GEOSTATIONARY SATELLITE IMAGER

Su Jeong Lee, Myoung-Hwan Ahn, Yeonjin Lee
Department of Atmospheric Sciences and Engineering,
Ewha Womans University, Seoul, Korea

Abstract

The Advanced Meteorological Imager (AMI), the main payload for the next generation Geostationary Korea Multi-Purpose Satellite (GEO-KOMPSAT-2A) planned to be launched in 2018, will have much improved spectral, temporal, and spatial resolution compared to the first generation imager. With the improvements, many of new value-added products are expected to be produced. Among the new products, atmospheric instability information is one of the important new possibilities with the pseudo sounding capability of AMI. Here, we present a new algorithm based on artificial neural network (ANN) and the training process using the theoretically estimated brightness temperature and corresponding instability. To check the feasibility of the ANN algorithm, the algorithm is applied to the actual SEVIRI (Spinning Enhanced Visible and Infrared Imager) data which has a comparable capability with AMI, and the preliminary results are quite promising.

1. Introduction

The Advanced Meteorological Imager (AMI) onboard the Geostationary Korea Multi-Purpose Satellite (GEO-KOMPSAT-2A) is designed to have an improved spectral, temporal, and spatial resolution compared to the first generation imager. For example, the number of channels will be increased at least three folds (from 5 to 16) while the spatial resolution will be 2 km for the 10 infrared channels and 1 km for 6 visible channels. Furthermore, the time required to scan a full disk will be reduced to about one-fifth of the current 28 minutes. With these improvements, many of new value-added products are expected to be produced, in addition to the significant improvement of the current 16 products.

Among the new products, atmospheric instability information is one of the important new possibilities with the pseudo-sounding capability of AMI. Although its accuracy is expected to be limited due to the limited number of sounding channels, its high spatial and temporal resolution could provide a significant addition for the nowcasting applications. In this study, we present a preliminary result from a new algorithm which is under development for AMI. The new algorithm is based on artificial neural network (ANN) which derives the instability information directly from the measured brightness temperatures (Tbs) instead of estimating the instability from the retrieved temperature (T) and humidity (q) profiles derived from retrieval algorithms such as variational, statistical, or physical approaches. The main reason to test an ANN algorithm is to reduce computational time and thus to keep the original high spatial and temporal resolution in the derived instability data.

To check the feasibility of the ANN algorithm, we selected the Convective Available Potential Energy (CAPE), which represents a column integrated atmospheric instability as the instability information. The backgrounds for the selection of CAPE is closely related with the information contents that the new imager channels have. Although those infrared channels are not capable of resolving high resolution vertical information of T and q, they carry a significant amount of information on the total column amount of water vapor and integrated temperature, even though weak information on the vertical profiles of T and q would limit the algorithm performance. To demonstrate

the feasibility, we use the theoretical Tbs simulated by a radiative transfer model with the input profiles of T and q derived from a hyperspectral sounding instrument, IASI (Infrared Atmospheric Sounding Interferometer) onboard Metop. We then prepare the training data set with the simulated Tbs and corresponding CAPE values estimated by the vertical profiles of T and q. We, then, apply the ANN algorithm to the actual SEVIRI (Spinning Enhanced Visible and Infrared Imager) observation data as the observation channels of SEVIRI are comparable with those of AMI.

2. Methodology

In general, the atmospheric instability information from the satellite observation is estimated from the retrieved vertical profiles of T and q. The so-called physical retrieval method is currently used for Meteosat Second Generation SEVIRI and GOES Sounder to derive stability information (EUMETSAT, 2013; Li et al., 2012). However, when applying this approach to retrieve vertical T and q profiles from imagery data with high resolution (such as data from AMI), one needs to reduce the spatial and temporal resolution of the data to lessen computational burden and to maximize signal to noise ratio. A good alternative is to statistically estimate the stability information directly from the measured radiances using an ANN with multilayer perceptron, which is known to be excellent to approximate highly nonlinear functions without prior knowledge of the relationship (Gardner and Dorling, 1998). Though it requires a large number of individual runs to determine the best solution, the retrieval can be made fast and often with surprising accuracy (Gardner and Dorling, 1998) once the statistical relations are established.

The overall flow of the algorithm training and its validation is schematically summarized in Figure 1. The primary inputs and the output for ANN training are theoretical Tbs and CAPE, respectively. CAPE is calculated from the vertical T and q profiles obtained from IASI and then objectively filtered to build a uniform data set for training (detailed description for data selection is provided in section 2.1). The selected CAPE values serve as the target outputs for training, and corresponding T and q profiles are used as input profiles for the radiative transfer model run to obtain radiances at the top of the atmosphere (TOA). Then, the simulated spectral radiances are band-averaged using the spectral response functions (SRF) for SEVIRI. Finally, the theoretical Tbs are obtained from the band-averaged radiances using the inverse of the Planck equation. The ANN training starts with the data set which consists of a combination of a number of inputs (Tbs, time, latitude, longitude, satellite zenith angle, etc.) and output (CAPE) and repeats the training until it obtains best solutions, i.e. until the errors between the ANN outputs and the target outputs are minimized. Once the train ends and the ANN parameters that lead to the best network results are determined, the algorithm can be applied to retrieve instability information (CAPE) directly from the measured radiance from a geostationary imager.

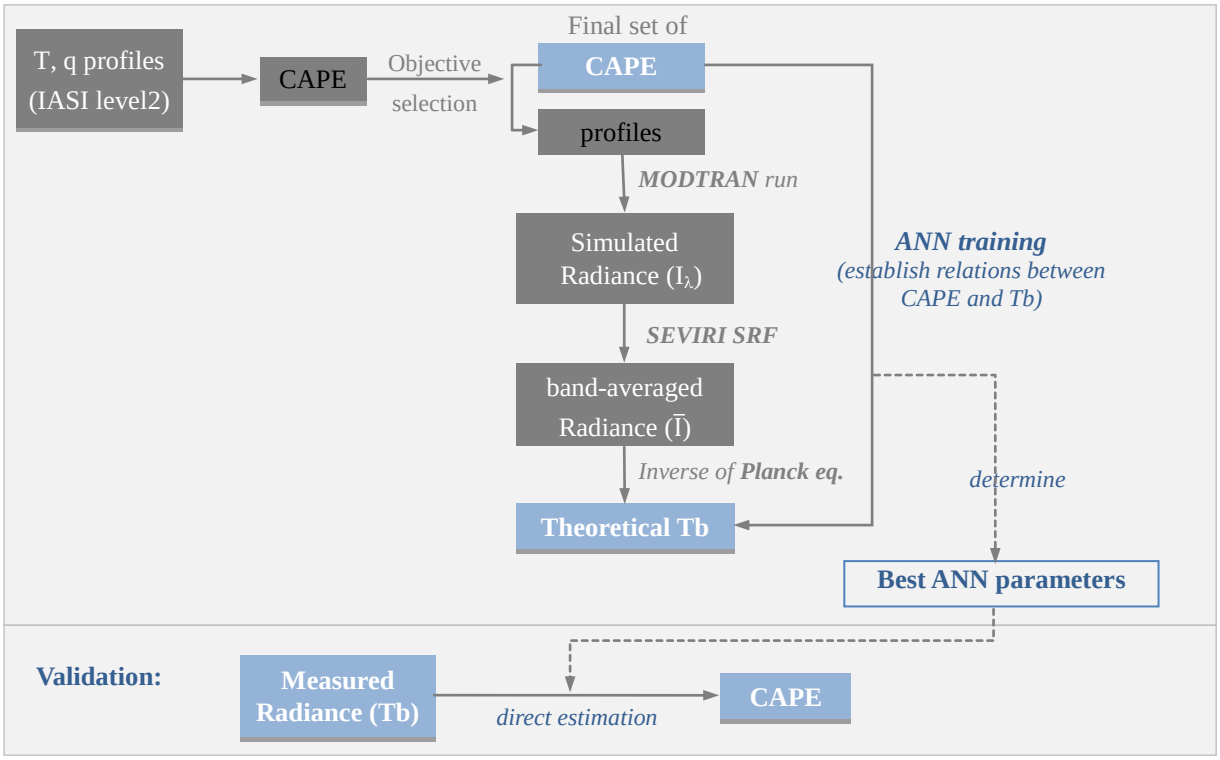

Figure 1 Flowchart for the overall process of the ANN training and validation to derive the atmospheric instability (CAPE) directly from the measured radiances of geostationary imagers

2.1 Data and Model

The T and q profiles of the IASI Level-2 products from January to December 2012 between 35N-75N latitude and 75W-75E longitude, obtained from EUMETSAT are used for the simulation of SEVIRI Tb. Around six days per month, six or seven consecutive orbits per day passing over the target area, total 449 orbits, are first selected and later additional 63 orbits, which include more severe weather events, are selected. Only the valid temperature and humidity data from cloud-free pixels are used for the calculation of CAPE. The distribution of CAPE calculated from the obtained T and q profiles are shown in the second column in Table 1. To construct a uniform set of training data as possible, the same amount of data (2,399) from three different CAPE ranges, total 7,197, was selected out of 63,877 profiles as shown in the third column of the table.

Table 1 Total and selected number of profiles

CAPE range	Total #	Selected #
occurrence of cape between 0 and 1000	53,600	2,399
occurrence of cape between 1000 and 2000	7,878	2,399
occurrence of cape over 2000	2,399	2,399
TOTAL	63,877	**7,197**

Then, the upwelling radiances at TOA for clear sky are simulated from those selected 7,197 profiles

using MODTRAN (MODerate resolution TRANsmission) version 5.2.2, which includes a very fine spectroscopy of spectral resolution 0.1 cm^{-1} ranging from 0 to 50,000 wavenumbers (Berk et al., 2011). The simulated radiances (R(λ)) are then weighted using the SEVIRI SRF (ϕ(λ)) to generate band-averaged radiances ($\overline{R}$) as given in equation (1), and then these band-averaged radiances are converted into corresponding Tbs using the inverse of Planck equation.

$$\overline{R} = \frac{\int_{\lambda_0-\Delta\lambda}^{\lambda_0+\Delta\lambda} R(\lambda)\phi(\lambda)d\lambda}{\int_{\lambda_0-\Delta\lambda}^{\lambda_0+\Delta\lambda} \phi(\lambda)d\lambda} \quad (1)$$

For the characterization and validation of the ANN model, SEVIRI 2.5 min (super) rapid scan data obtained on 20 June, 2013 is used. The number (or type) of required input variables for the retrieval should be the same as those used for training. Thus, Tbs from the seven IR channels (WV 6.2, WV 7.3, IR 8.7, IR 9.6, IR 10.8, IR 12.0, and IR13.4), satellite zenith angle, latitude, longitude, time and day information are used to retrieve CAPE using the ANN algorithm.

2.2 Artificial Neural Network (ANN)

The Multi-Layer perceptron feedforward back-propagation algorithm is used to find the relation between the simulated Tbs and CAPE and to retrieve CAPE directly from the measured Tbs. Figure 2 shows the structure of the neural network used for this study. It consists of three layers of one input layer with 12 input variables (circular time, circular day, latitude longitude, satellite zenith angle, and simulated Tbs), one hidden layer with 12 neurons, and one output layer with one obvious output neuron, i.e., CAPE. Time and day are converted into circular forms (Blackwell and Chen, 2009) using $x(t) = cos\ \frac{2\pi t}{24}$ for time and $y(t) = cos\ \frac{2\pi t}{365}$ for day to treat the discontinuity problem near t = 0 and t = 24 for time and t = 1 and t = 365 for day. The hyperbolic tangent function, which generally leads to faster convergence (Blackwell and Chen, 2008), is used as the activation function in the hidden layer while in the output layer, the weighted inputs to the output neuron are just summed and do not pass through an activation function.

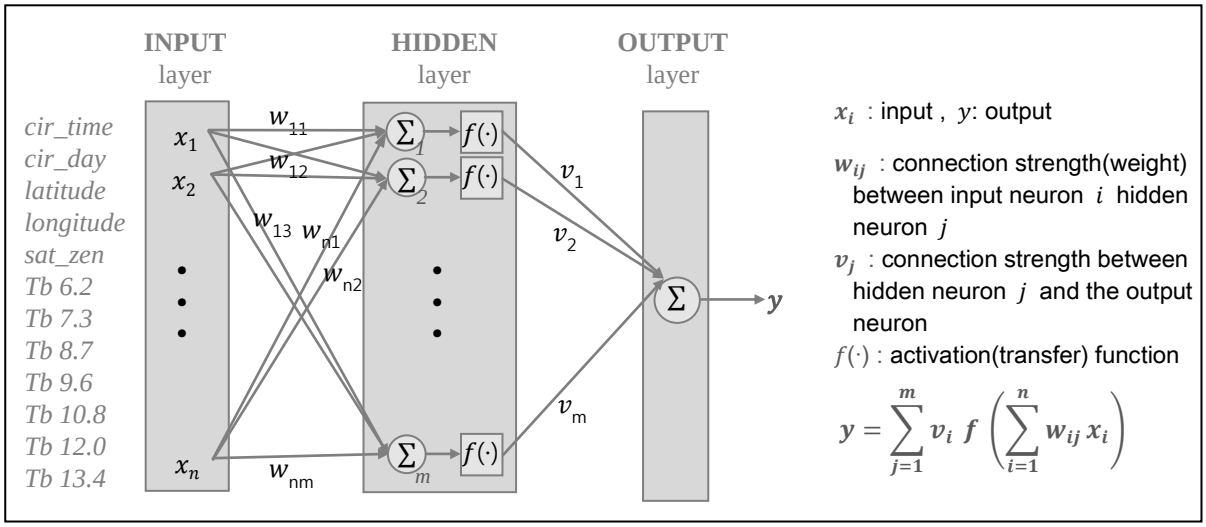

Figure 2 Multilayer perceptron feedforward backpropagation algorithm

For each training pattern (i.e., a set of input variables), the bias between the target and the retrieved output values for the pattern is calculated, and this bias is used to update the weights between the hidden and output layers first, and again this newly updated weights are used to update the weights

between the input and hidden layers. Thus, the weights between layers are updated in the direction in which the error (or bias) decreases most rapidly (Blackwell and Chen, 2009), and the network fitness is evaluated by the root mean square error (RMSE) which is given by (2) for every iteration (epoch).

$$RMSE = \sqrt{\frac{\sum_p (y_{target}{}^{(p)} - y^{(p)})^2}{\#\ of\ pattern}} \qquad p: pattern\ (sample\ size) \qquad (2)$$

3. RESULTS

3.1 Network training with IASI data

Before the real training process begins, the network randomly selects or divides the training dataset into three different groups for training, testing, and validation with a user-defined proportion, e.g., 60-20-20. However, careful monitoring of this selection process revealed that the random function does not work properly in many cases, repeatedly assigning particular data or patterns (e.g. CAPE values smaller than 1,000) to a particular group, eventually resulting in a poor retrieval performance. Thus, the network-selected patterns in each group need to be monitored first before starting network-training to make sure patterns are uniformly assigned to three different groups. To avoid this issue, the 7,197 IASI data are manually divided into three groups with 80-10-10 split in this study so that all three different groups include a comprehensive data set as possible.

The three important ANN parameters that determine the algorithm performance, i.e. the number of hidden neurons, number of epochs, and learning rate, are also manually adjusted. While changing the number of hidden neurons between 11 and 13, the number of epochs between 1,000 and 5,000 with an interval of 1,000, and the learning rate between 0.05 and 0.95 with an interval of 0.05, the change of errors (RMSE) in the training, testing, and validation data sets are monitored. After going through a number of training processes, the combination of ANN parameters that leads to the best retrieval performance was determined as: 12 hidden neurons, 3000 epochs (iteration) and the learning rate of 0.3. The retrieved CAPE obtained with this combination of ANN parameters are compared with the target values in Figure 3. The correlation between the two is around 0.90 with the mean absolute error (average of absolute errors) of 330 and RMSE of 438.

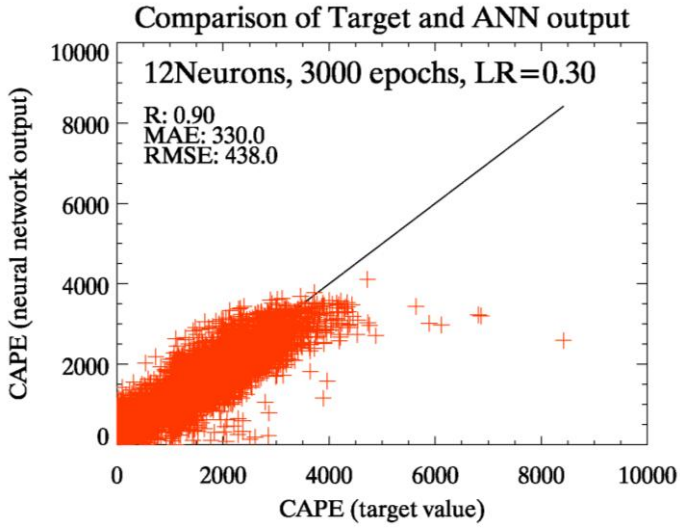

Figure 3 Scatter plot of the ANN-derived CAPE versus the respective target values (IASI) used in the training data set

Analysis of the weight change between the input-hidden and hidden-output layers for a particular input variable reveals the degree to which the input variable contributes to the final output. For easy comparison, the weights associated with the connection from an input to the neurons in the hidden layer are multiplied by the corresponding weights between the hidden neuron and the output neuron and then linearly summed. Figure 4 depicts how the neural network changes the weights of each input variable as the number of epochs increases. In this specific case, the weights, which are initially given as small random values, rapidly increase for Tb8.7 and Tb9.6 and decrease for Tb12.0 and Tb13.4 until the iteration reaches around 300 and then repeat minor changes. Meanwhile the weights for the other input variables show slight or little changes through the whole training process. However, with a different set of input variables, the network behaves differently. In a train with Tb10.8 - Tb12.0 instead of Tb12.0 (all the other inputs are the same as in the previous case), the overall magnitude of weights decreases and the weights associated with Tb10.8 - Tb12.0 and Tb7.3 gradually increase throughout the training process (Figure 5). Thus, further investigation needs to be done to reveal the contribution of each variable to the final output.

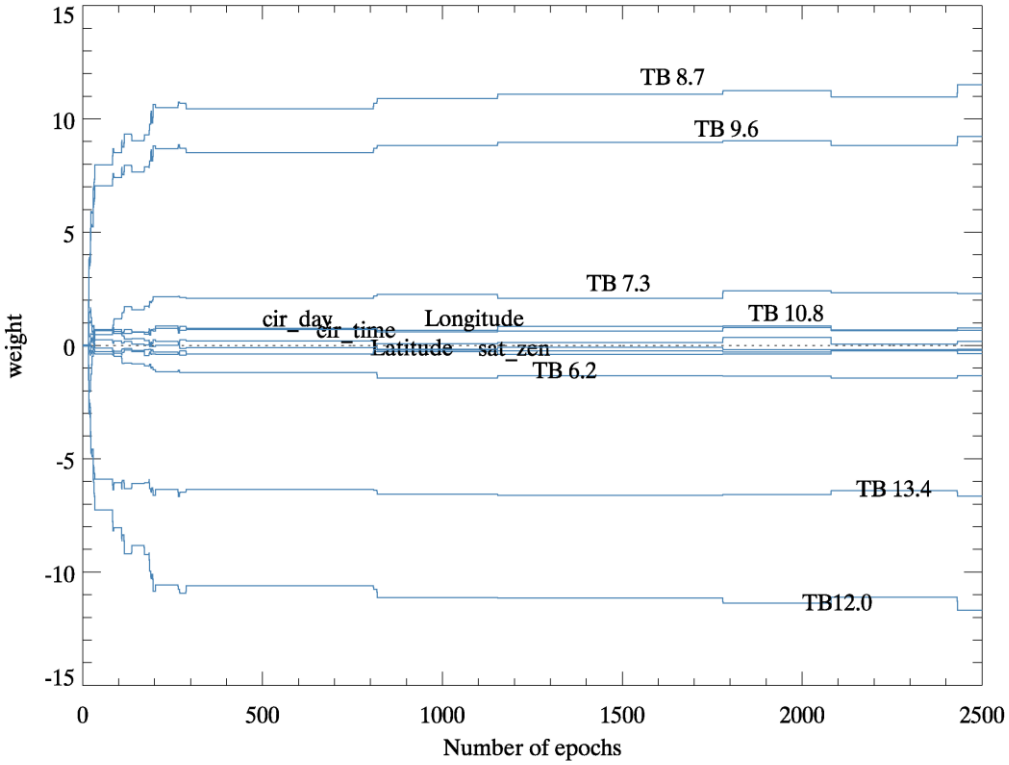

Figure 4 Weight changes for each input variable with increasing epochs when training with 12 inputs of circular day, circular time, latitude, longitude, satellite zenith angle, TB6.2, TB7.3, TB8.7, TB9.6, TB10.8, TB12.0 and TB 13.4

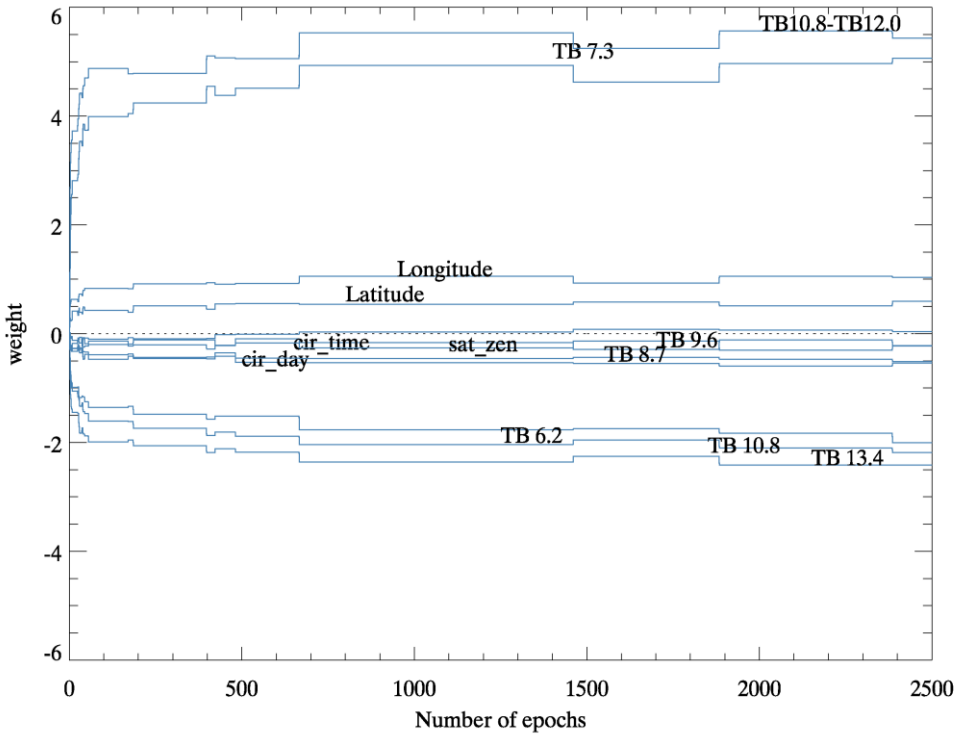

Figure 5 Weight changes for each input variable with increasing epochs when training with the same inputs as in Figure 4 except TB10.8-TB12.0 instead of TB12.0

The final weights associated with each input variable that lead to the best network performance, i.e., the weights at the end of the training process, are displayed in Figure 6. Only the strongest connection between the input and the hidden neurons is plotted and the thickness of arrows indicates the magnitude of weight. As already shown in the analysis of weight trend, among 12 input variables, Tbs particularly Tb8.7 and Tb12.0 are identified as discriminating input measurements, having strong connections with the neurons in the hidden layer (also shown in Table 2).

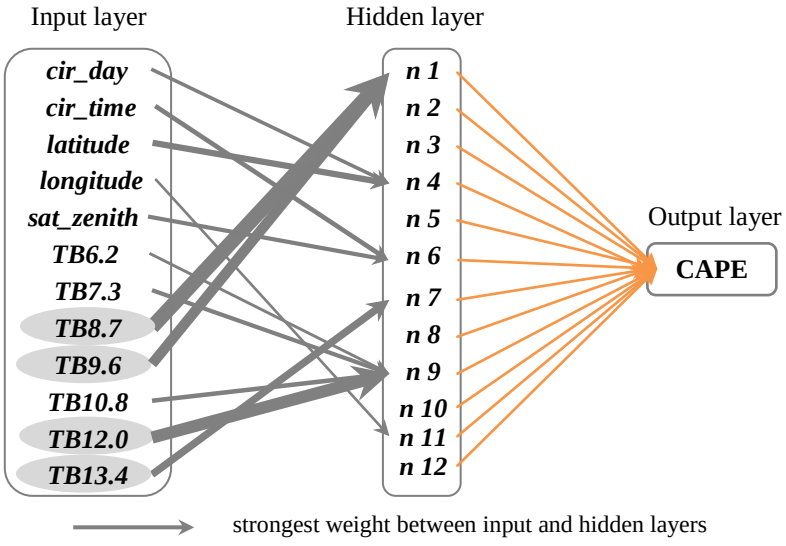

Figure 6 final combination of weights that results in the best network performance (The thickness of arrows between input and hidden layers indicates the magnitude of weight)

Table 2 Final weights between input and hidden layers for each input variable, and weight between the hidden and output layers (only the strongest weight between the input and hidden layers is included in the table)

Input	**Strongest weight** (associated hidden neuron)	**Hidden neuron**	**Weight to output neuron**
cir_day	1.35 (n4)	n1	0.29
cir_time	-1.75 (n6)	n2	-0.46
Latitude	-2.34 (n4)	n3	-0.14
longitude	-0.75 (n11)	n4	0.20
sat_zenith	1.57 (n6)	n5	0.30
TB 6.2	1.10 (n9)	n6	0.15
TB 7.3	-1.58 (n9)	n7	-0.22
TB 8.7	5.52 (n1)	n8	-0.22
TB 9.6	3.90 (n1)	n9	-0.23
TB 10.8	1.69 (n9)	n10	-0.14
TB 12.0	4.56 (n9)	n11	-0.05
TB 13.4	2.78 (n7)	n12	-0.45

3.2 CAPE derived using ANN algorithm

The retrieval algorithm is applied to actual satellite data obtained during the SEVIRI 2.5 minute rapid scan test carried out with the Meteosat-8 satellite (Setvák and Müller, 2013). Selected date is 20 June, 2013 when severe convective storms developed over Europe. Seven brightness temperatures mentioned above and five other parameters (latitude, longitude, day, time, and satellite zenith angle) from the rapid scan data are fed into the algorithm as inputs. To retrieve CAPE for clear-sky condition, retrieval process is conducted only for the pixels with Tb10.8 greater than 273 K, Tb10.8 - Tb12.0 greater than 0 K, Tb10.8 - Tb8.7 greater than 0 K, and Tb10.8 - Tb6.2 greater than 40 K.

The retrieved CAPE values plotted over the Tb10.8 images from morning to evening hours are shown in Figure 7 in 2-hour time interval from (a) to (f). Several significant features are found from the retrieved results. First, during the afternoon hours (at around 13:02 UTC) several convective clouds begin to pop up over the regions where the CAPE values are relatively high at 09:02 UTC image (marked with arrows and circles) and developed to the severe convective clouds (at 15:02 UTC). Another significant feature is that high CAPE values around the leading edges of clouds induce a further development, while weaker CAPE values around the trailing edges result in weakened convective activities. However, no significant convection occurs over high CAPE areas in the morning images (at around 11:02 UTC marked with dashed blue arrows) which requires further investigation.

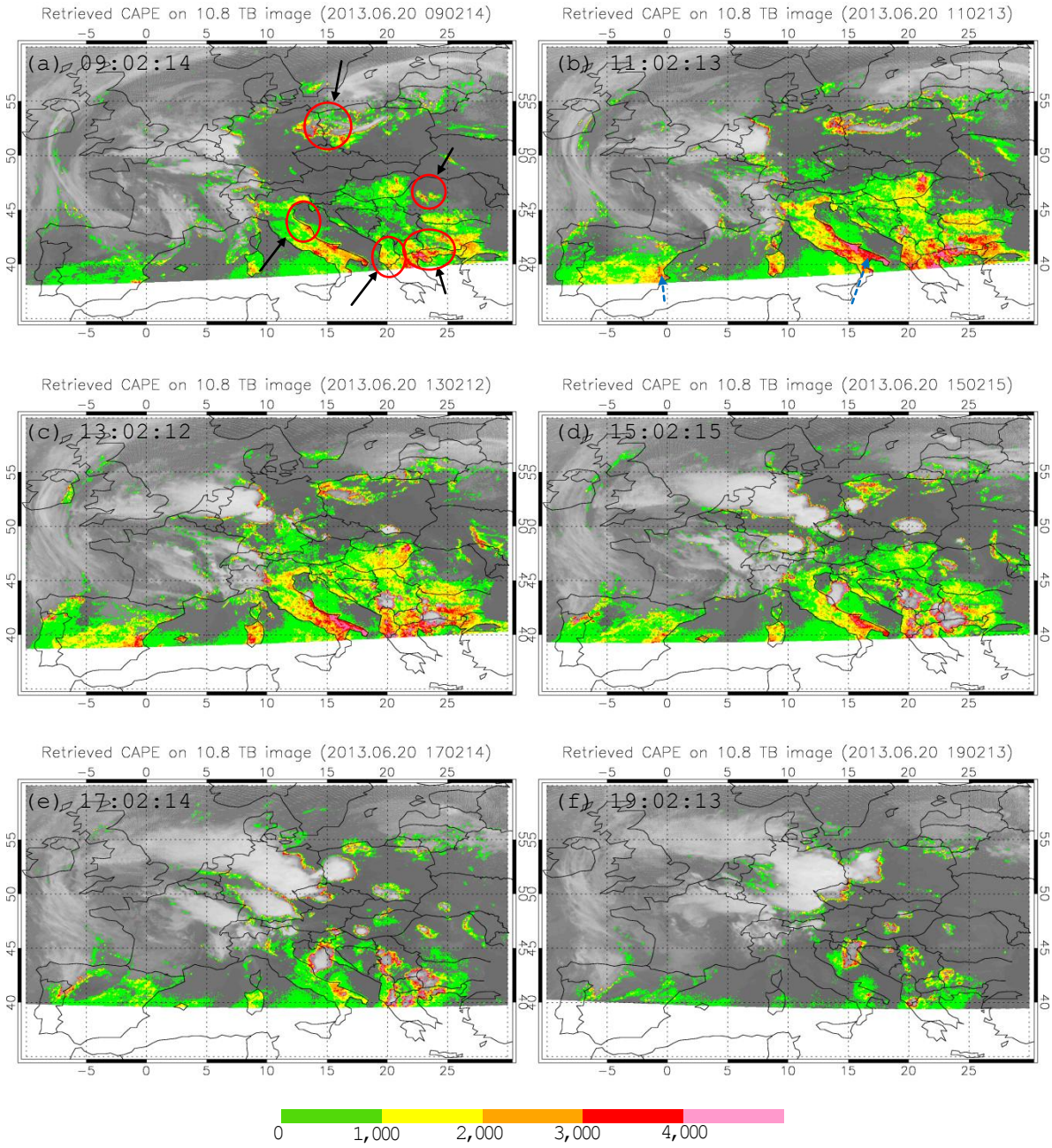

Figure 7 Retrieved CAPE from SEVIRI 2.5 min rapid scan data using the ANN algorithm trained with the theoretically prepared training dataset.

4. Conclusions

The current study introduces a new method for retrieving atmospheric instability indices directly from the measured radiances of imagery data based on ANN approach. With the careful preparation of the training data set to represent the situation as comprehensive as possible and the selection of proper ANN parameters, it is shown that the trained algorithm could fit the training data set quite satisfactorily. Although the retrieved results using the actual observation data raise the need for further investigation and refinement of the proposed algorithm, it is shown that an ANN algorithm cloud be

used to derive the convective potential of the atmosphere in the major convective areas. To increase its validity, a comprehensive validation with the well-established observation such as the radiosonde or analysis field from a numerical weather prediction model is planned. Also, application of the current algorithm to different cases and quantitative validation are going to be conducted.

Acknowledgments

We would like to give special thank to Marianne Koenig at EUMETSAT for the technical support and guidance. This research was funded by the National Meteorological Satellite Center (NMSC) titled "A Study on the Development of Meteorological Data Processing Techniques of Geostationary Meteorological Satellite".

References

Berk, A., G.P. Anderson, P. K. Acharya, and E. P. Shettle, 2011: MODTRAN® 5.2.2 User's Manual, Spectral Sciences, Inc., MA, 5-6

Blackwell W. J. and F. W. Chen, 2009: *Neural Networks in Atmospheric Remote Sensing*, Boston, MA:Artech House, 78-85, 125-127

EUMETSAT, 2013: ATBD for the MSG GII/TOZ Product, EUMETSAT, EUM/MET/DOC/11/0247

Gardner, M. W. and Dorling, S. R., 1998: Artificial Neural Networks (the Multilayer Perceptron): a review of applications in the atmospheric sciences. *Atmos. Env*., 32, 2627-2636

Koenig, M. and E. D. Coning, 2008: The MSG Global Instability Indices Product and Its Use as a Nowcasting Tool. *Weather and Forecasting*, 24, 272-285

Li J., T. J. Schmit, X. Jin, G. Martin, 2012: GOES-R Advanced Baseline Imager (ABI) algorithm theoretical basis document for legacy atmospheric moisture profile, legacy atmospheric temperature profile, total precipitable water, and derived atmospheric stability indices. NOAA/NESDIS/STAR, (July), 11-12

Setvák, M. and J. Müller, 2013: 2.5-minute rapid scan experiments with the MSG satellites. Paper presented at *the 7th European Conference on Severe Storms*, Helsinki, Finland. 3-7 June 2013